

Development of a Technique for Determining Young's Modulus of Vertically Aligned Carbon Nanotubes Using the Nanoindentation Method

O. A. Ageev, O. I. Il'in, A. S. Kolomiitsev, B. G. Konoplev,
M. V. Rubashkina, V. A. Smirnov, and A. A. Fedotov

Taganrog Institute of Technology, Southern Federal University, Taganrog, 347928 Russia

e-mail: ttismirnov@gmail.com

Received August 10, 2011

Abstract—A technique for determining Young's modulus of vertically aligned carbon nanotubes using the refined micromechanical model of the nanoindentation of a forest of vertically aligned carbon nanotubes is developed. The results of experimental studies of Young's modulus determination for vertically aligned carbon nanotubes with different geometrical parameters are given. It is shown that, for a forest of carbon nanotubes with an effective diameter of around 100 nm and an effective length of approximately 2 μm , as well as for a forest with an effective diameter of carbon nanotubes of roughly 52 nm and their effective length of nearly 500 nm, the values of Young's modulus are 1.68 ± 0.08 and 1.01 ± 0.05 TPa, respectively. Our results can be used for developing the technological processes of the formation of structures for nano- and microelectronics and nano- and microsystem technology on the basis of vertically aligned carbon nanotubes.

DOI: 10.1134/S1995078012010028

INTRODUCTION

The development trends of modern science and technology show that progress in nanotechnologies will lead to significant breakthroughs in fields such as electronics, medicine and public health, energetics, biotechnologies, information technologies, etc. [1]. In recent years, modern nanotechnological equipment has been developed which allows one to accomplish urgent tasks for the formation of nanoscale structures and minimize the time it takes to carry out the technological, interoperational, and checking-measuring procedures, as well as their costs [2].

Both single-walled and multiwalled vertically aligned carbon nanotubes (VACNTs) belong to a promising class of nanomaterials whose unique electrical, chemical, and mechanical properties can be actively used for the development and creation of new devices for nano- and microelectronics, as well as nano- and microsystem technology [3]. However, it is necessary for this purpose to carry out a more detailed study of their properties, both electrophysical and physico-mechanical ones.

An analysis of published data has shown that Young's modulus (one of the basic physical-mechanical parameters of carbon nanotubes (CNTs)) has a significant spread of values over a range of 0.4–6.85 TPa (Table 1). Moreover, the experimentally obtained values of Young's modulus of CNTs are 2–3 times smaller [4–9] than the theoretical values calculated for this parameter [10–12]. This may be associated with the

fact that Young's modulus of CNTs strongly depends on the CNT wall thickness, whose value in practice is almost an order of magnitude greater than the calculated theoretical values [13].

The application of traditional experimental methods for determining Young's modulus (the direct tensile load, the pulse dynamic method, etc.) is complicated due to the dimensions of the investigated structures and also because of the necessity of consolidating the nanotubes on the substrate. Therefore, the development of alternative techniques for determining Young's modulus of CNTs to control their parameters is an urgent task.

One of the most promising methods for determining Young's modulus of VACNTs is a nanoindentation test based on indenting the diamond needle (indenter) into the surface of the VACNT forest and receiving the resulting load curve (the dependence of the depth of the indenter penetration into the forest upon the indentation force) [9]. This method requires neither complicated preparation, the fastening of the sample, nor the application of additional specialized analytical equipment.

The main disadvantage of the technique based on the micromechanical model for determining the mechanical properties of CNTs using nanoindentation [9] is that the bending stiffness parameter, from which the Young's modulus of the CNT is then calculated, serves as a fitting parameter for the theoretical dependences of the depth of the indenter penetration

Table 1. Summary table of the values of Young's modulus of CNTs

Method for CNT manufacturing	Method for determining elastic properties	CNT diameter, nm	CNT length, μm	Young's modulus, TPa	Reference
Carbon-arc discharge method	Raman spectroscopy for monitoring the deformations of CNTs embedded in an epoxy matrix	10–20	—	1.7–2.4	[1]
	Direct tensile loading	8.5–19.4	1.49–7.97	0.62–1.2	[2]
	Theory of beams (fixed at one end), atomic force microscopy (AFM)	26–76	—	1.28	[3]
	Analysis of thermal vibrations on the basis of the theory of continuous beams using transmission electron microscope (TEM)	5.6–24.8	0.66–5.81	0.4–4.15	[4]
	Measuring the resonant frequency using the counterelectrode and high-frequency excitation	12–40	1.5–6.25	1	[5]
PECVD, Ni catalysts	Beam theory, nanoindentation	55–104	0.57–1.15	0.91–1.24	[6]
Theoretical calculation based on different methods	Methods of band theory; wall thickness of CNT $t = 0.071 \text{ nm}$	—	—	5.1	[7]
	Methods of molecular dynamics; wall thickness of CNT $t = 0.08 \text{ nm}$	—	—	6.85	[8]
	Finite element methods; wall thickness of CNT $t = 0.075 \text{ nm}$	—	—	4.84	[9]

in the VACNT forest upon the applied indentation force to match them with the experimental dependences, which considerably reduces the reliability of this technique.

This work is aimed at developing a technique for determining Young's modulus on the basis of refining the micromechanical model of nanoindentation, as well as at investigating the influence of the geometrical parameters of VACNTs on their mechanical properties.

EXPERIMENTAL PROCEDURE

Two forests of VACNTs, which were grown using plasma-enhanced chemical vapor deposition (PECVD) from the gas phase at the NANOFAB NTK-9 multifunctional nanotechnological complex (manufactured by ZAO Nanotechnology-MDT, Zelenograd, Russia) [1, 3, 14], were used as the experimental samples.

An investigation into the geometric parameters of the obtained VACNTs (diameter, length, and density) was carried out using a Nova NanoLab 600 scanning electron microscope (SEM) (FEI, the Netherlands). Figure 1 presents the resulting SEM images, an analysis of which has shown that, for the first forest, the effective CNT diameter D_1 is around 100 nm, the effective CNT length L_1 is roughly 2 μm , and the average areal density of CNTs in the forest m_1 is approximately $30 \mu\text{m}^{-2}$; for the second forest, the effective CNT diameter D_2 is roughly 52 nm, the effective CNT

length L_2 is around 0.5 μm , and the average areal density of CNTs in the forest m_2 is approximately $34 \mu\text{m}^{-2}$.

The investigation in VACNT mechanical properties was conducted at the NTEGRA Vita Probe Nanolaboratory by means of a scanning hardness nanotester integrated in it [14]. A diamond three-sided Berkovich pyramid with an apex angle of $\theta = 70^\circ$ between the edge and height was used as the indenter.

In the course of nanoindentation, the diamond probe was indented into the sample surface at a constant speed; the process was accompanied by recording the values of the load and the appropriate depth of indenter penetration in the material, on the basis of which the resulting dependence (load curve) was plotted [15].

The schematic process of the nanoindentation of a VACNT forest is shown in Fig. 2. Initially, the indenter is in position close to the top of the forest (Fig. 2a), then, with the application of a load, the mechanical interaction between the indenter and the forest surface occurs when the displacing indenter encounters the first CNT at the depth h_1 (Fig. 2b); with a further increase in the load, the first nanotube begins to suffer bending deformation while the indenter touches the second tube at the depth h_2 (Fig. 2c). At the given depth h , the indenter interacts with i CNTs, each of which is deflected by a certain distance w_0 (Fig. 2d), depending on the initial depth of the contact of the

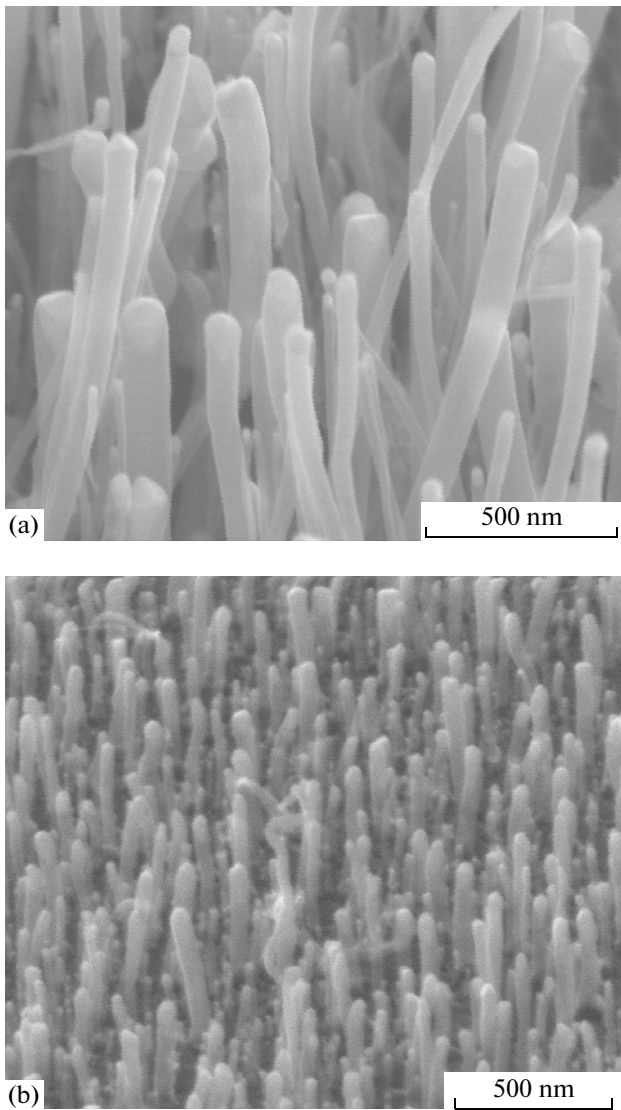


Fig. 1. SEM images of VACNT forests used in experimental studies: (a) the first forest and (b) the second forest.

indenter with the i th tube and on the indenter geometry [9]:

$$w_0 = (h - h_i) \tan \theta. \quad (1)$$

At the same time, the nanoindentation process can be regarded using the micromechanical model. This model is based on the beam theory, according to which an individual vertically aligned nanotube is an elastic hollow cylindrical rod fixed at one end (see Fig. 2c). In this case, the elastic deflection w of the CNT, having the outer diameter D and the length L , with an external load application is described by the equation [9]

$$(EI)_{\text{eff}} \frac{d^2 w}{dx^2} = Tx + P(w_0 - w), \quad (2)$$

where $(EI)_{\text{eff}}$ is the effective bending stiffness of the CNT and P and T are the forces acting on a nanotube in parallel and perpendicular directions relative to its axis, respectively.

The solution to Eq. (2) describes the dependence of the individual nanotube deflection on the appropriate bending stiffness and applied load [9]:

$$w_0 = \frac{T}{P} \left(\frac{\tan kL}{k} - L \right), \quad (3)$$

where $k = \sqrt{P/(EI)_{\text{eff}}}$ is the coefficient.

The bending stiffness of a CNT is a product of Young's modulus of the CNT and its effective moment of inertia I_{eff} . If a CNT is regarded as a hollow cylindrical rod, then the tube's moment of inertia is equal to $I_{\text{eff}} = \pi(D^4 - D_i^4)/64 \approx \pi D^4/64$, where D_i is the CNT's inner diameter [9].

Whence Young's modulus of an individual CNT can be calculated as

$$E \approx \frac{64(EI)_{\text{eff}}}{\pi D^4}. \quad (4)$$

Thus, the value of the bending stiffness parameter must be determined for Young's modulus calculation. In [9], by plotting the theoretical load curves (on the basis of Eqs. (1) and (3)) and fitting these curves through the parameter $(EI)_{\text{eff}}$ to the experimental curves obtained using nanoindentation, the authors

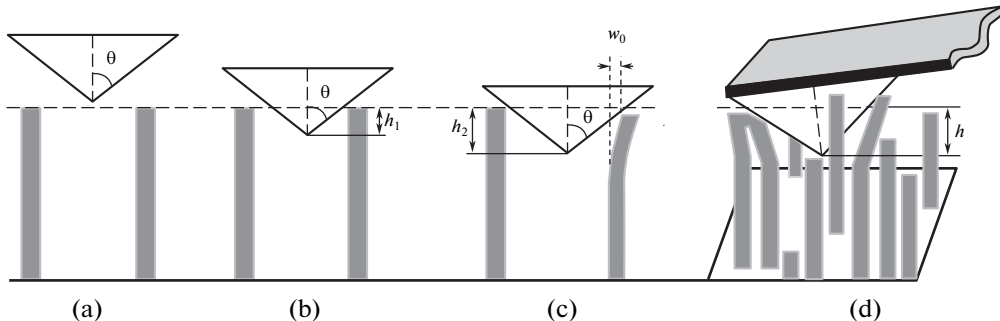


Fig. 2. Schematic of nanoindentation of the VACNT forest: (a) the indenter in the position close to the top of the forest, (b) the indenter touches the first nanotube, (c) the deflection of the first CNT with the load increase and the indenter interaction with the second tube, and (d) the indenter interaction with i CNTs at the depth h .

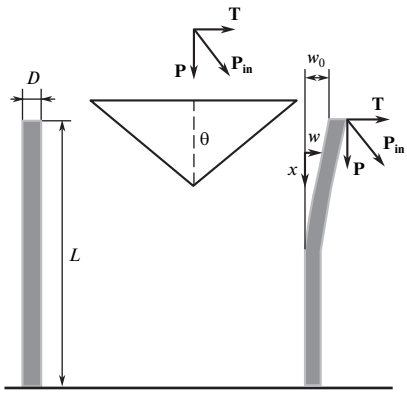


Fig. 3. Schematic of the process of indenter interaction with VACNTs described by the refined micromechanical model.

chose a value of the bending stiffness $(EI)_{\text{eff}}$ based on the best correlation of the two curves; i.e., the bending stiffness played the role of a fitting parameter.

A method for assessing the bending stiffness $(EI)_{\text{eff}}$ of each i th tube interacting with the indenter directly from the experimental load curves has been proposed as a refinement of the micromechanical model. For this purpose, the force P acting on a single CNT was represented as

$$P = (P_{\text{in}} - P_i) \cos \theta / i, \quad (5)$$

where P_{in} is the indentation force being a sum of the forces P and T (Fig. 3); P_i is the indentation force, which corresponds to the depth h_i , at which the indenter touches the i th tube; and i is the number of nanotubes interacting with the indenter under the load P_{in} . The values of the forces P_{in} and P_i are determined from the experimental curves obtained in the process of the nanoindentation of the VACNT forest (Fig. 4).

Thus, Young's modulus is calculated from the following expression:

$$E = \frac{64(P_{\text{in}} - P_i)\cos\theta}{\pi i D^4 k^2}. \quad (6)$$

The number i of nanotubes interacting with the indenter under the specified load is defined as a product of the indenter's total interaction area S at the penetration depth h and the VACNT forest density m . The total area S is a sum of the indenter's cross section area S_{ind} at the depth h , the area of interaction along the indenter's perimeter S_{per} , and the cross section area of the nanotube itself S_{CNT} . Due to the fact that the Berkovich indenter is a regular three-sided pyramid with an apex angle of $\theta = 70^\circ$, the height of the triangle which lies at the base of this pyramid is calculated from the formula

$$a = 1.5h \tan 70^\circ,$$

while the edge of the base is expressed as

$$c = 2a \tan 30^\circ.$$

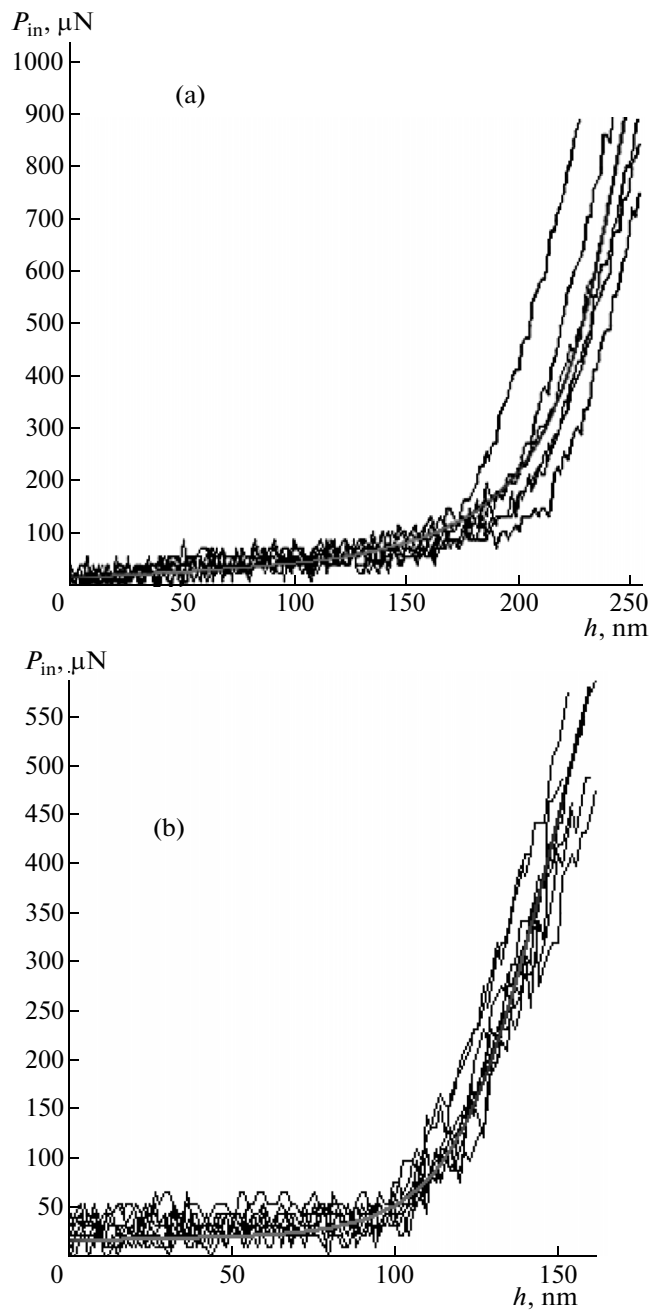


Fig. 4. The experimental load curves (dark lines) obtained during the nanoindentation of the VACNT forest and the averaged load curves (red lines) for the (a) first and (b) second VACNT forests.

Whence the area S of the indenter interaction with a single tube at the penetration depth h is equal to

$$\begin{aligned} S &= i/m = S_{\text{ind}} + S_{\text{per}} + S_{\text{CNT}} \\ &= 9.853h^2 + 14.355hD_0 + 3.141D_0^2/4. \end{aligned} \quad (7)$$

Equation (7) makes it possible to determine not only the number of tubes interacting with the indenter at the depth h , but also the depth h_i , at which the indenter touches the i th tube.

Table 2. The modes of nanoindentation process and the calculated values of mechanical parameters for the first VACNT

CNT number <i>i</i>	<i>S</i> , μm^2	<i>h_i</i> , nm	<i>P_i</i> , μN	<i>(EI)_i</i> , N nm^2	<i>E_i</i> , TPa
1	0.033	16	5	7.77	1.58
2	0.068	34	11	7.84	1.59
3	0.099	48	18	7.68	1.56
4	0.135	62	21	8.10	1.65
5	0.165	73	25	8.32	1.69
6	0.201	85	32	8.25	1.68
7	0.233	95	36	8.63	1.75
8	0.267	105	43	8.55	1.74
9	0.303	115	50	8.59	1.75
10	0.333	123	56	8.61	1.75
11	0.369	132	63	8.82	1.79
12	0.402	140	71	8.12	1.65
13	0.436	148	78	8.70	1.77
Average value:				8.30 ± 0.38	1.68 ± 0.08

RESULTS AND DISCUSSION

The nanoindentation process was carried out with the application of loads of 1000 and 550 μN at eight different points about 9 μm from each other for the first and second VACNT forests, respectively. Figure 4 demonstrates the experimental dependences and the averaged load curves, which were drawn according to the obtained statistical data for the first and second VACNT forests.

An analysis of the presented curves has shown that the dependence of the depth of the indenter penetration into the VACNT forest upon the indentation force is nonlinear. The curve can be divided into two parts: the region of elastic interaction (from 0 to 150 nm for the first forest and from 0 to 100 nm for the second one) and the inelastic interaction region (from 150 to 250 nm for the first forest and from 100 to 150 nm for the second one).

The micromechanical model describes only small elastic deflections; therefore, for the calculation of Young's modulus of the CNT, only the first region of the curve was used. On this basis, the total depth *h* of the indenter penetration into the first forest was 150 nm, that of its penetration into the second forest was 100 nm, and the respective indentation forces were around 80 and 50 μN ; in this case the number *i* of the nanotubes interacting with the indenter at the depth *h* is 14 and 6 respectively.

A calculation of Young's modulus of a CNT was performed with the use of a refined micromechanical model (Eqs. (5), (7), (8)). The values of Young's modulus for each *i*th tube interacting with the indenter at the depth *h* for the first and second forests are presented in Tables 2 and 3, respectively. The obtained average values of Young's modulus of the VACNT,

amounting to 1.68 ± 0.08 and 1.01 ± 0.05 TPa, correlate well with the data from [4–9] presented in Table 1.

The difference between the values of Young's modulus for the first and second VACNT forests may be related to the influence of VACNT geometric parameters on Young's modulus. On the one hand, the number of inner layers of multiwalled CNTs increases as the effective diameter of the VACNT grows. As the results of nanoindentation modeling for multiwalled VACNT [13] show, the growth in the number of layers of multiwalled CNTs has a significant impact on the value of Young's modulus of the CNT due to the increase in the van der Waals interaction between adjacent layers and because of the additional resistance of a CNT to bending deformations during the indentation. On the other hand, the CNT resistance to bending deformations decreases as its length increases, similarly to the behavior of a beam in the classical elasticity theory. As a result, the partial compensation of influence of these parameters on the value of Young's modulus of CNTs may occur in case of the simultaneous reduction in diameter and length of nanotubes in the second VACNT forest relative to those in the first forest.

Thus, our technique can be successfully utilized for measuring the mechanical properties of VACNTs using the nanoindentation method and also for investigating the effect of geometrical parameters of VACNTs on their Young's modulus.

Limits of the applicability of the described technique are determined by the aspect ratio of CNTs in the VACNT forest and the nanotube deflection during the application of an external load in the process of nanoindentation. The maximum value of CNT deflection during the nanoindentation, at which the indenter interaction with a VACNT forest can be still

Table 3. The modes of nanoindentation process and the calculated values of mechanical parameters for the second VACNT

CNT number <i>i</i>	<i>S</i> , μm^2	<i>h_i</i> , nm	<i>P_i</i> , μN	<i>(EI)_i</i> , N nm^2	<i>E_i</i> , TPa
1	0.029	27	20	0.302	0.983
2	0.059	47	23	0.315	1.027
3	0.086	62	26	0.336	0.937
4	0.118	77	30	0.388	1.081
5	0.149	90	40	0.372	1.036
Average value:				0.34 ± 0.04	1.01 ± 0.05

described by the beam-bending theory, depends on the CNT length and is defined by the following expression:

$$w_{\max} = (0.2L - h_l)\tan\theta, \quad (8)$$

where $0.2L$ is the maximum penetration depth determined from the experimental dependences (see Fig. 4).

The rigidity of CNT fixing on the substrate surface does not significantly influence the results of investigations and is not a limiting factor for the developed technique, because the total depth of the indenter penetration into the VACNT forest doesn't exceed 20% of the length of a nanotube (see Fig. 4).

From an analysis of our experimental data, we can conclude that the minimum ratio of the length of the investigated CNT to its diameter at which the CNT can be considered an elastic beam should be 10 : 1. In order to refine the limits of applicability of this technique, it is necessary to carry out additional studies.

CONCLUSIONS

As a result of this work, a technique was developed for measuring the mechanical properties of VACNTs using the nanoindentation method; the micromechanical model of nanoindentation of a VACNT forest was refined which made it possible to pass from the Young's modulus calculation using the fitting parameter, as determined from the correlation of theoretical and experimental load curves, to the calculation of Young's modulus directly from the experimental curves obtained during the nanoindentation. This refinement allows one to determine the values of Young's modulus of CNTs in a VACNT forest with a higher degree of reliability owing to the possibility of obtaining the statistical data set and its subsequent processing, which is unique to this technique. In addition, this technique differs from others in that it requires no special preparation of VACNT forests after their growth, which suggests the potential possibility of using this technique as a rapid-technique for inter-operational control in the manufacture of vacuum electronic devices.

The developed technique was used for experimental investigations in the influence of geometric parameters of the VACNTs on their Young's modulus. The

obtained values of Young's modulus of CNTs correlate well with the published data, which confirms the reliability of the developed technique.

The obtained results may be applied for the development of the technological processes of formation of structures for nano- and microelectronics and for nano- and microsystem technology based on vertically aligned forests of carbon nanotubes, while this technique may be used for determining the mechanical properties of nanotubes and filiform nanocrystals (nanowires) made of other materials, which requires additional study.

REFERENCES

1. B. Bhushan, *Springer Handbook of Nanotechnology*, 3rd ed. (Springer, 2010).
2. V. A. Bykov and O. A. Ageev, "Technological Equipment for Creation of Nanosystem Technique," *Nanotekhnol. Ekol. Proizvodstvo*, No. 5, 68–70 (2010).
3. O. A. Ageev, O. I. Il'in, V. S. Klimin, A. S. Kolomiitsev, and A. A. Fedotov, "Research Modes of the Formation and Modification Oriented Arrays of Carbon Nanotubes by PECVD on Nanotechnological Complex NANOFAB NTK-9," *Izv. YuFU, Tekh. Nauki*, No. 4, 69–77 (2011).
4. O. Lourie and H. D. Wagner, "Evaluation of Young's Modulus of Carbon Nanotubes by Micro-Raman Spectroscopy," *J. Mater. Res. B* **13**, 2418 (1998).
5. W. Ding, L. Calabri, K. M. Kohlhaas, X. Chen, D. A. Dikin, and R. S. Ruoff, "Modulus, Fracture Strength, and Brittle vs. Plastic Response of the Outer Shell of Arc-Grown Multi-Walled Carbon Nanotubes," *Exp. Mech.* **47**, 25–36 (2007).
6. E. W. Wong, P. E. Sheehan, and C. M. Lieber, "Nanobeam Mechanics: Elasticity, Strength, and Toughness of Nanorods and Nanotubes" *Science* **277** (5334), 1971 (1997).
7. M. M. J. Treacy, T. W. Ebbesen, and J. M. Gibson, "Exceptionally High Young's Modulus Observed for Individual Carbon Nanotubes," *Nature* **381** (6584), 678 (1996).
8. P. Poncharal, Z. L. Wang, D. Ugarte, and W. A. Heer, "Electrostatic Deflections and Electromechanical Resonances of Carbon Nanotubes," *Science* **283** (5407), 1513 (1999).
9. H. J. Qi, K. B. K. Teo, K. K. S. Lau, M. C. Boyce, W. I. Milne, J. Robertson, and K. K. Gleason, "Deter-

- mination of Mechanical Properties of Carbon Nanotubes and Vertically Aligned Carbon Nanotube Forests using Nanoindentation," *J. Mech. Phys. Solids* **51**, 2213 (2003).
10. X. Zhou, J. J. Zhou, and Z. C. Ou-Yang, "Strain Energy and Young's Modulus of Single-Wall Carbon Nanotubes Calculated from Electronic Energy-Band Theory," *Phys. Rev.* **62**, 13692 (2000).
11. X. Chen and G. Cao, "A Structural Mechanics Approach of Single-Walled Carbon Nanotubes Generalized from Atomistic Simulation," *Nanotechnology* **17**, 1004 (2006).
12. A. Pantano, D. M. Parks, and M. C. Boyce, "Mechanics of deformation of single- and multi-wall carbon nanotubes," *J. Mech. Phys. Solids* **52**, 789 (2004).
13. L. Liu, G. Cao, and X. Chen, "Mechanisms of Nanoindentation on Multiwalled Carbon Nanotube and Nanotube Cluster," *J. Nanomaterials* **2008**, Article ID 271763 (2008).
14. <http://www.ntmdt.ru>
15. K. V. Gogolinskii, N. A. L'vova, and A. S. Useinov, "Application Scanning Probe Microscopes and Nano-hardness Meters for Studying the Mechanical Properties of Solid Materials at a Nanolevel," *Zavod. Lab. Diagn. Mater.* **73** (6), 28–36 (2007).

SPELL: ok